Coherent mechanical noise cancellation and cooperativity competition in optomechanical arrays

de Jong, Matthijs H.J.; Li, Jie; Gartner, C.M.; Norte, Richard A.; Gröblacher, Simon

DOI
10.1364/OPTICA.446434

Publication date
2022

Document Version
Final published version

Published in
Optica

OPTICA

Coherent mechanical noise cancellation and cooperativity competition in optomechanical arrays

Matthijs H. J. de Jong,[1,2,†] Jie Li,[1,3,†] Claus Gärtner,[1] Richard A. Norte,[2] and Simon Gröblacher[1,*]

[1]Kavli Institute of Nanoscience, Department of Quantum Nanoscience, Delft University of Technology, Lorentzweg 1, 2628CJ Delft, The Netherlands
[2]Department of Precision and Microsystems Engineering, Delft University of Technology, Mekelweg 2, 2628CD Delft, The Netherlands
[3]Zhejiang Province Key Laboratory of Quantum Technology and Device, Department of Physics, Zhejiang University, Hangzhou 310027, China
*Corresponding author: s.groeblacher@tudelft.nl

Received 19 October 2021; revised 15 December 2021; accepted 10 January 2022; published 2 February 2022

Studying the interplay between multiple coupled mechanical resonators is a promising new direction in the field of optomechanics. Understanding the dynamics of the interaction can lead to rich new effects, such as enhanced coupling and multi-body physics. In particular, multi-resonator optomechanical systems allow for distinct dynamical effects due to the optical cavity coherently coupling mechanical resonators. Here, we study the mechanical response of two SiN membranes and a single optical mode, and find that the cavity induces a time delay between the local and cavity-transduced thermal noises experienced by the resonators. This results in an optomechanical phase lag that causes destructive interference, cancelling the mechanical thermal noise by up to 20 dB in a controllable fashion and matching our theoretical expectation. Based on the effective coupling between membranes, we further propose, derive, and measure a collective effect, cooperativity competition on mechanical dissipation, whereby the linewidth of one resonator depends on the coupling efficiency (cooperativity) of the other resonator.

https://doi.org/10.1364/OPTICA.446434

1. INTRODUCTION

Cavity optomechanics [1] addresses the interaction between electromagnetic fields and mechanical motion. In recent years, multi-mode optomechanics, such as multiple mechanical resonators interacting with a common cavity field, has received significant attention and offered a platform for studying rich physics, including hybridization [2–5] and synchronization [6–8] of mechanical modes, mechanical state swapping [9], coherent [10] and topological [11] energy transfer, and two-mode squeezed mechanical states [12–14]. In particular, optomechanical systems consisting of multiple SiN membranes have seen considerable progress towards the enhancement of their single-photon coupling rate [15–18], and have been the subject of many theoretical proposals [19–23]. Compared to the relatively simple description of the standard optomechanical system, arrays of mechanical resonators coupled to a common optical mode offer the prospect of studying complex new physical effects and the ability to achieve individual control over each constituent of a multi-element system.

In this work, we study two mechanical resonators, coherently coupled to a common cavity mode that couples the thermal mechanical noise of the two resonators in an effective mechanical beam-splitter interaction [22,24] that can be used to swap the mechanical states [9,25] or topologically transfer energy between them [11]. By operating in the side-band unresolved regime, the optomechanically scattered photons that mediate this effective mechanical beam-splitter interaction can remain coherent in the cavity, which adds a stochastic time delay to this process. This results in a time delay in the effective (local and transduced) noise experienced by each resonator, which causes destructive interference when the mechanical resonator spectra overlap. We measure up to 20 dB cancellation of mechanical noise, matching well with our theoretical model. This provides a new interference mechanism distinct from that attributed to direct mechanical coupling between two resonators [2,26], to multiple optical modes [27,28] or optical modulation [29], which can clearly be excluded in our system.

We further propose and derive another new collective effect, resulting in a cooperativity competition of the mechanical dissipation, which we also observe in our measurements. This competition arises between the dissipation dynamics of two mechanical resonators coupled to the same optical field and leads to a linewidth broadening of one resonator that depends on the optomechanical cooperativity of the other resonator.

2. THEORY AND EXPERIMENTAL SETUP

Our system consists of an array of two nominally identical 200 nm thick SiN membranes [Fig. 1(a)] with fundamental frequencies $\omega_{1,2} \simeq 2\pi \times 150$ kHz and linewidths $\gamma_{1,2} \simeq 2\pi \times 0.1$ Hz. They are patterned with a photonic crystal with 35% reflectivity at 1550 nm [30], characterized in a previously described

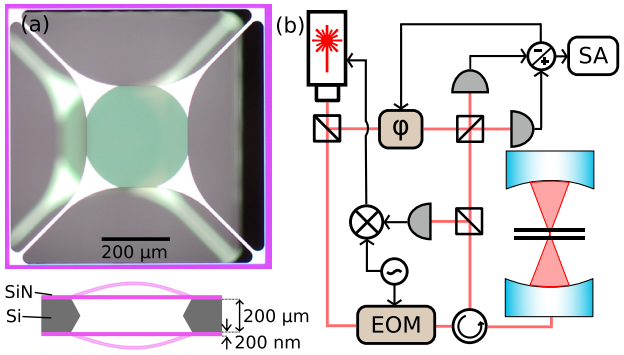

Fig. 1. (a) (top) Microscope image of a double-membrane device. (bottom) Cross-section of the double-membrane chip, with the SiN membranes on either side of the Si substrate. The 200 μm spacing between the two membranes is rigid, fixed by the substrate. (b) Schematic of the experimental setup. The laser wavelength is locked to the cavity length using a Pound–Drever–Hall locking scheme, and the mechanics of the membranes are measured via homodyne detection. SA, Spectrum analyzer; φ, Fiber stretcher; EOM, Electro-optic modulator.

setup [31]. The double-membrane chip is placed close to the center of a 49.6 mm long Fabry–Perot cavity (free spectral range 3.023 GHz, beam waist 33 μm), with an empty-cavity optical linewidth (full width at half maximum) of $\kappa_e = 2\pi \times 128$ kHz, in principle putting us into the optomechanical sideband resolved regime (total linewidth $\kappa \lesssim \omega_j$). The membranes cause additional optical loss when placed inside the cavity due to scattering and small imperfections in the alignment, resulting in a linewidth $\kappa \gtrsim 2\pi \times 300$ kHz, with a strong dependence on the exact position [32] and alignment [30] of the membranes. The mechanical motion of the membranes is coupled to the optical cavity frequency ω_c with vacuum optomechanical coupling rates $g_{0,1}$ and $g_{0,2}$ respectively. A laser at frequency ω_ℓ is coupled to the cavity with coupling strength $E = \sqrt{P_\ell \kappa_e/\hbar\omega_\ell}$, where P_ℓ is the laser power and κ_e the external coupling rate of the cavity.

The behavior of the membranes is investigated using a homodyne detection setup, schematically shown in Fig. 1(b), for which we lock the laser wavelength ($\lambda = 1549.62$ nm) to the cavity length using a Pound–Drever–Hall (PDH) locking scheme [33]. By tuning the parameters of our PID controller, we can lock the laser beam slightly off-resonant with our cavity, and the red (blue) detuned laser can be used to cool (amplify) our optomechanical system.

The Hamiltonian describing our system is given by

$$\hat{H}/\hbar = \omega_c \hat{a}^\dagger \hat{a} + \sum_{j=1,2} \left(\frac{\omega_j}{2} \left(\hat{x}_j^2 + \hat{p}_j^2 \right) - g_{0,j} \hat{a}^\dagger \hat{a} \hat{x}_j \right) + iE \left(\hat{a}^\dagger e^{-i\omega_\ell t} - \text{H.c.} \right), \tag{1}$$

with $\hat{a}$ ($\hat{a}^\dagger$) the annihilation (creation) operator of the cavity mode, and $\hat{x}_j$ and $\hat{p}_j$ the dimensionless position and momentum of the j^{th} mechanical resonator. We are interested in the fast fluctuations of the mechanical operators ($\delta\hat{x}_j$, $\delta\hat{p}_j$) and optical field, which are described by the quantum Langevin equations (QLEs, see Supplement 1 Sec. 1 for details)

$$\begin{aligned} \delta\dot{\hat{x}}_j &= \omega_j \delta\hat{p}_j \\ \delta\dot{\hat{p}}_j &= -\omega_j \delta\hat{x}_j - \gamma_j \delta\hat{p}_j + G_j^* \delta\hat{a} + G_j \delta\hat{a}^\dagger + \hat{\xi}_j \\ \delta\dot{\hat{a}} &= -(i\Delta + \kappa/2)\,\delta\hat{a} + i \sum_{j=1,2} G_j \delta\hat{x}_j + \sqrt{\kappa}\hat{a}^{\text{in}}, \end{aligned} \tag{2}$$

where $\hat{\xi}_j$ and $\hat{a}^{\text{in}}$ are the mechanical and optical noise terms. We have further introduced an effective detuning $\Delta = \omega_c - \omega_\ell - \sum_j \frac{g_{0,j}^2}{\omega_j} |\langle\hat{a}\rangle|^2$ and the effective optomechanical coupling rate $G_j = g_{0,j}\langle\hat{a}\rangle = g_{0,j} E/(\kappa/2 + i\Delta)$, with $\langle\hat{a}\rangle$ being the average cavity field amplitude. We can solve these equations by taking the Fourier transform and deriving the expected power spectral density (PSD) detected from the cavity output field (Supplement 1 Sec. 2).

3. RESULTS

A. Interference from Optomechanical Phase Lag

In this section, we introduce of the optomechanical phase lag, and show that it leads to interference in the dynamics of the two mechanical resonators. To simplify the following analysis, we take the phase of $\langle\hat{a}\rangle$ such that the G_j are real (the full derivation keeping any complex values of G_j is given in Supplement 1 Sec. 1). If we solve the QLEs [Eq. (2)], the position fluctuations for resonator 1, for example, take the form

$$\delta\hat{x}_1 = \chi_1^{\text{eff}}(\omega) \left\{ \frac{-G_1 G_2 [\chi_c(\omega) - \chi_c^*(-\omega)]\chi_2(\omega)\hat{\xi}_2 + iG_1\sqrt{\kappa}[\hat{a}^{\text{in}}\chi_c(\omega) + \hat{a}^{\text{in},\dagger}\chi_c^*(-\omega)]}{i + G_2^2\chi_2(\omega)[\chi_c(\omega) - \chi_c^*(-\omega)]} + \hat{\xi}_1 \right\}, \tag{3}$$

where we have introduced the natural susceptibility of the mechanical resonators, $\chi_j(\omega) = \frac{\omega_j}{\omega_j^2 - \omega^2 - i\gamma_j\omega}$, and of the cavity field, $\chi_c(\omega) = \frac{1}{\kappa/2 + i(\Delta - \omega)}$ ($\chi_c^*(-\omega) = \frac{1}{\kappa/2 - i(\Delta + \omega)}$), and an effective susceptibility that incorporates the optomechanical effects on the susceptibility of the mechanical resonator,

$$\chi_1^{\text{eff}}(\omega) = \left[\frac{1}{\chi_1(\omega)} + \frac{G_1^2 \left(\chi_c(\omega) - \chi_c^*(-\omega) \right)}{i + G_2^2 \chi_2(\omega) \left(\chi_c(\omega) - \chi_c^*(-\omega) \right)} \right]^{-1}. \tag{4}$$

Equation (3) features terms that contain the different noise sources, the optical noises $\hat{a}^{\text{in}}$, $\hat{a}^{\text{in},\dagger}$, and the mechanical noises of both resonators, $\hat{\xi}_1$, $\hat{\xi}_2$. If we neglect the optical noises, which is a valid assumption if the system is at room temperature, we can see that the position fluctuations of the resonator depend on an effective mechanical noise, $\hat{\xi}^{\text{eff}}$,

$$\hat{\xi}_1^{\text{eff}}(\omega) = \hat{\xi}_1 + M_1\hat{\xi}_2, \quad \hat{\xi}_2^{\text{eff}}(\omega) = \hat{\xi}_2 + M_2\hat{\xi}_1 \tag{5}$$

with

$$\begin{aligned} M_1(\omega) &= \frac{i\chi_2(\omega) G_1 G_2 \left(\chi_c(\omega) - \chi_c^*(-\omega) \right)}{1 - iG_2^2\chi_2(\omega)(\chi_c(\omega) - \chi_c^*(-\omega))} \\ M_2(\omega) &= \frac{i\chi_1(\omega) G_1 G_2 \left(\chi_c(\omega) - \chi_c^*(-\omega) \right)}{1 - iG_1^2\chi_1(\omega)(\chi_c(\omega) - \chi_c^*(-\omega))}. \end{aligned} \tag{6}$$

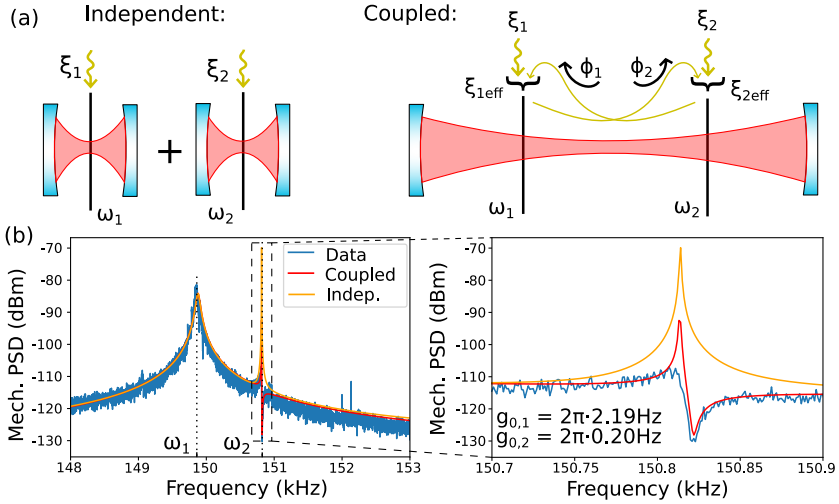

Fig. 2. (a) Schematic of mechanical noise contribution for two independent (left) or cavity-coupled (right) resonators. (b) Measured mechanical spectra for two membranes in a single cavity, where one membrane (ω_1) is significantly stronger coupled (more damped) than the other (ω_2). Theory models are fitted for the independent (uncoupled) and the coupled membranes case, including optomechanical phase lag.

This is the crucial point: The position fluctuations of any (one) of the two resonators are not only dependent on its local thermal bath, but also on the thermal bath of the other via the optical field [Fig. 2(a)], as is well-understood for general coupled resonators [34]. This cross-term between the resonators is the effective mechanical beam-splitter interaction used for state swapping and energy transfer between the mechanical resonators [9,11,22,24,25]. It represents photons that have been scattered with phonon transfer (i.e., optomechanically scattered) from one resonator, and subsequently re-scattered from the other. While this is a second-order optical process, it is linear in the mechanical operators, so it is not eliminated by the linearization of the QLEs [Eq. (2)]. We quantify the rate of this process in Supplement 1 Sec. 3, and show that the transduced noise can be similar in amplitude to the local noise.

To evaluate these expressions and obtain a PSD such as the one we detect in our experimental setup, conventionally, one assumes each of the mechanical baths to be Markovian (if $Q_j = \frac{\omega_j}{\gamma_j} \gg 1$ [35,36]), with autocorrelators for $\hat{\xi}_j$ as

$$\left\langle \hat{\xi}_j(t)\hat{\xi}_j(t') + \hat{\xi}_j(t')\hat{\xi}_j(t) \right\rangle /2 \approx \gamma_j(2\bar{n}_j + 1)\delta(t - t'), \qquad (7)$$

with $\bar{n}_j$ the mean thermal phonon number (Supplement 1 Sec. 4). Based on Eq. (5), we can write an autocorrelator for the effective noise, which will contain terms from both thermal baths.

It is here that we introduce new physics. In Eq. (5), both noises have an *immediate* effect on the position fluctuations of the resonator: $\delta\hat{x}_1(t)$ is dependent on $\hat{\xi}_1(t)$ and $\hat{\xi}_2(t)$. For the local noise, this is correct, but the transduced noise must have a finite time delay due to the separation of the resonators (thermal baths) and the non-zero travel time of the photons between them: $\delta\hat{x}_1(t)$ must depend on $\hat{\xi}_1(t)$ and $\hat{\xi}_2(t - \bar{t})$ for an average photon travel time $\bar{t}$. The well-established framework of Eq. (2) breaks down: it does not contain this time delay. It predicts an immediate response of, e.g., resonator 1 when resonator 2 is moved, regardless of the finite photon travel time. Note that the noise transduced by the cavity is first experienced by the other resonator from its own thermal bath [Fig. 2(a)].

We introduce the time delay of the transduced noise with respect to the local noise in the autocorrelation of the effective thermal noise experienced by a resonator (e.g., resonator 1),

$$\begin{aligned}
&\langle \hat{\xi}_1^{\text{eff}}(t)\hat{\xi}_1^{\text{eff}}(t') + \hat{\xi}_1^{\text{eff}}(t')\hat{\xi}_1^{\text{eff}}(t)\rangle/2 \\
&= \left\langle \left(\hat{\xi}_1(t) + M_1(t) * \hat{\xi}_2(t)\right)\left(\hat{\xi}_1(t') + M_1(t') * \hat{\xi}_2(t')\right)\right\rangle \\
&\Rightarrow \left\langle \left(\hat{\xi}_1(t) + M_1(t) * \hat{\xi}_2(t - \bar{t})\right)\left(\hat{\xi}_1(t') + M_1(t') * \hat{\xi}_2(t' - \bar{t})\right)\right\rangle,
\end{aligned} \qquad (8)$$

where $M(t) = \mathcal{F}^{-1}\{M_1(\omega)\}$ from the inverse Fourier transform, the time delay between the local and transduced noise is $\bar{t}$, and $*$ denotes convolution. We have explicitly introduced the delay time $\bar{t}$ only in the transduced noise term; by property of the convolution, we could have distributed the time delay freely between $M_1(t)$ and $\hat{\xi}_2(t)$ without affecting the result. In the frequency domain, using the time-shift property of the Fourier transform, we get a phase shift,

$$\begin{aligned}
&\langle \hat{\xi}_1^{\text{eff},'}(\omega)\hat{\xi}_1^{\text{eff},'}(\omega') + \hat{\xi}_1^{\text{eff},'}(\omega')\hat{\xi}_1^{\text{eff},'}(\omega)\rangle/2 \\
&= \left\langle \left(\hat{\xi}_1(\omega) + e^{-2i\pi\bar{t}\omega} M_1(\omega)\hat{\xi}_2(\omega)\right)\right. \\
&\quad \left. \times \left(\hat{\xi}_1(\omega') + e^{-2i\pi\bar{t}\omega} M_1(\omega')\hat{\xi}_2(\omega')\right)\right\rangle,
\end{aligned} \qquad (9)$$

where we have denoted the effective noise with added time delay by $\hat{\xi}_j^{\text{eff},'}$. The frequency range of interest is close to the mechanical frequencies ($\omega \sim \omega_1 \simeq \omega_2$), so we can consider it as a constant phase factor $e^{-2i\pi\bar{t}\omega} \simeq e^{i\phi_1}$. We call this the *optomechanical phase lag* that the transduced noise experiences with respect to the local noise. This modifies Eq. (5) to

$$\hat{\xi}_1^{\text{eff},'}(\omega) = \hat{\xi}_1 + \alpha_1 e^{i\phi_1} M_1 \hat{\xi}_2, \quad \hat{\xi}_2^{\text{eff},'}(\omega) = \hat{\xi}_2 + \alpha_2 e^{i\phi_2} M_2 \hat{\xi}_1, \qquad (10)$$

where we have introduced the amplitude fit factors α_1 and α_2 to account for imperfect alignment between the two membranes.

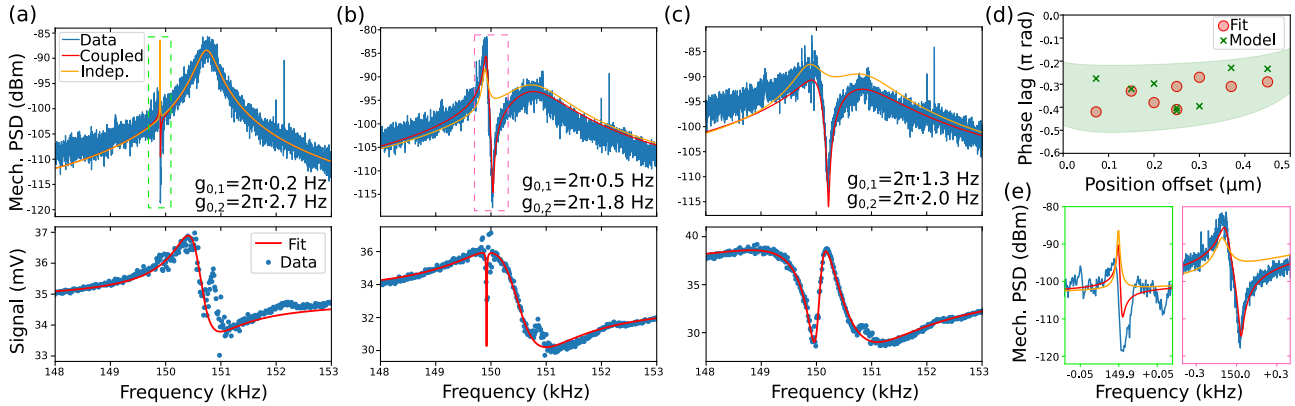

Fig. 3. (a)–(c) Top panels: Measured PSD for the two-membrane system for various coupling ratios (blue), and the expected behavior with interference (red) and considering independent membranes (orange). The measured coupling rates are shown, their ratios being 0.07, 0.28, and 0.65, respectively. Bottom panels: OMIT data (blue dots) and fits (red line) used to extract the optomechanical parameters. (d) Extracted phase lag from the fit (red circles) and expected phase lag based on the cavity linewidths (green crosses). The green shaded area shows the phase lag bounds based on the cavity linewidths, see main text. (e) Zoom-in on dashed regions of (a) and (b) showing narrow spectral features at the mechanical frequency of the less-coupled resonator.

Some closer considerations of this time delay and phase lag are warranted. An optomechanically scattered photon traveling the distance between resonators 1 and 2 (200 μm) takes about 670 fs, which should be negligible on the time scale of the mechanical motion, so we would expect the phase lag to be negligibly small as well. However, due to the optical cavity and the fact that $g_{0,j}$ is small, the chance for a scattered photon to directly interact with the other resonator is very small. It is much more likely to exit the cavity without interacting with the other membrane, as $\kappa \gg g_{0,j}$. The photons that do interact with the other membrane (i.e., the ones that have not exited the cavity) will thus have an average travel time equal to the lifetime of the cavity $\bar{t} = \tau = 1/\kappa$. In the regime $\kappa \simeq \omega_j$, this time lag represents a significant fraction of the mechanical period, meaning that the contributions to the effective noise of a resonator can be perfectly out of phase. When that happens, the effective noise term that resonator 1 experiences is reduced due to the coupling to resonator 2 and its thermal bath (and vice-versa). In other words, the local noise and the noise transduced by the optical field from the other resonator interfere. We estimate the optomechanical phase lag for systems from the literature (Supplement 1 Sec. 5) and distinguish interference due to this effect from other interference mechanisms (Supplement 1 Sec. 6).

B. Experimental Observation of Interference

We study the behavior of our optomechanical system by measuring the mechanical PSD with our homodyne setup. This allows us to test the theory curves obtained with the inclusion of the time delay and the curves obtained for two completely independent membranes (i.e., G_j set to zero while $G_{i\neq j} \neq 0$, for either membrane with the resulting spectra summed), shown in Fig. 2(b). As these measurements are in the frequency domain, we shall refer to the optomechanical phase lag rather than the time delay.

The theory curve for the independent resonators (orange, solid line) clearly shows two Lorentzians, one at ω_1 which is broadened due to optomechanical cooling, and one which is less coupled at ω_2 and therefore less broad. The theory curve with the added optomechanical phase lag (red, solid line) follows the other theory curve for most of the frequency domain: because the Lorentzian at ω_2 is narrow, the noise contribution from $\hat{\xi}_2$ to $\hat{\xi}_1^{\text{eff}}$ is only relevant for a small frequency range around ω_2 (inset). Here, the interference between the noise terms results in a characteristic Fano lineshape [37] in the theory curve where the spectra of the individual mechanical resonators would overlap.

Comparing both theory curves to the experimental data (blue, solid line), we see a clear drop in the PSD around ω_2, which the theory that includes the optomechanical phase lag describes well while the model without it does not. Note that the peak of the Fano lineshape is absent from the experimental data as well, which we attribute to experimental imperfections.

To further study how this interference based on the optomechanical phase lag behaves, we adjust the optomechanical coupling rates of the resonators. This changes the frequency range over which the interference is observable, and also its strength. By varying the position of the chip within the cavity, the optical field intensity that each membrane experiences is changed, which allows us to control the optomechanical coupling rate of each of the membranes. We consider four cases, one shown in Fig. 2(b) ($g_{0,1} \gg g_{0,2}$) and three in Figs. 3(a)–3(c), $g_{0,1} \ll g_{0,2}$, $g_{0,1} < g_{0,2}$, and $g_{0,1} \simeq g_{0,2}$. For the latter three, we also show optomechanically induced transparency (OMIT) measurements and fits [38–40] (for details see Supplement 1 Sec. 7), by which we independently obtain all optomechanical parameters. In these OMIT measurements [Figs. 3(a)–3(c), bottom row], we observe an additional feature not captured by our fit. Due to its frequency, it likely stems from the resonator's thermal noise.

In the case where one of the resonators has very weak coupling to the optical field, as shown in Figs. 2(b) and 3(a), the PSD of the more strongly coupled resonator takes the expected Lorentzian form. At the frequency of the weakly coupled resonator, we observe a consistent dip in the PSD [Figs. 2(b) right panel and 3(e)], where the noise drops $15-20$ dB below the level of the spectrum of the other mode. The optomechanical parameters [$\omega_1 = 2\pi \times 149.89$ kHz, $\omega_2 = 2\pi \times 150.80$ kHz, $\kappa \simeq 2\pi \times 600$ kHz, $\Delta = 2\pi \times 10$ kHz, $g_{0,1} = 2\pi \times 2.2$ Hz, and $g_{0,2} = 2\pi \times 0.2$ Hz for Fig. 2(b)] are also obtained through the separate OMIT measurement and fit.

When one of the resonators is less coupled, but not very weakly [Figs. 3(b) and 3(e)], we see a clear Fano lineshape in the PSD. If

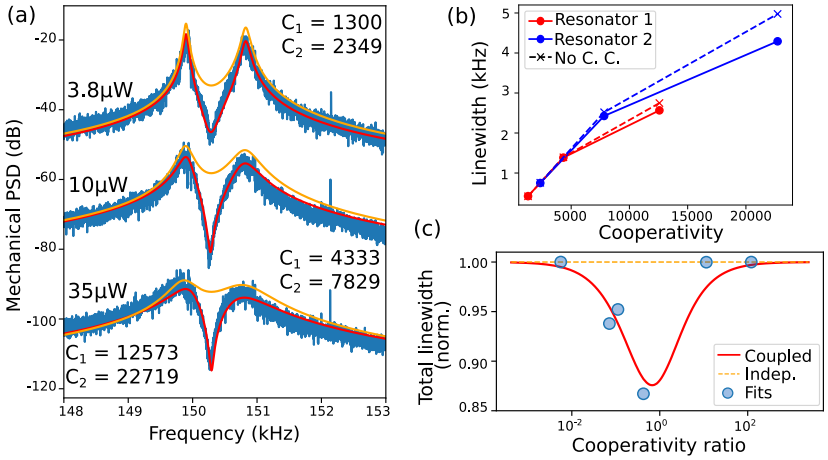

Fig. 4. (a) PSD for a fixed $g_{0,1}/g_{0,2} = 0.74$ and various powers (blue), with theory fits for the coupled-resonator (red) and independent-resonator models (orange). (b) Fitted mechanical linewidths as a function of cooperativity. Solid lines include the effect of cooperativity competition while dashed lines do not. (c) Normalized total (sum) linewidths for various coupling ratios (blue), showing a decrease due to cooperativity competition.

both resonators are approximately equally coupled [cf. Fig. 3(c)], the measured spectrum exhibits a pronounced anti-resonance [41], clearly signaling destructive interference. There is an additional mode at 147 kHz that is not included in the fits in Fig. 3. Combined, these measurements show that our model with phase lag consistently describes the experimental data much better (20 dB, a factor 100 difference) than the theory without the phase lag.

The most important factor governing the phase lag is the cavity linewidth κ. As we change the position of the chip in the cavity, κ changes due to scattering and misalignment losses. We plot the expected phase lag as a function of the chip position in Fig. 3(d) by way of the fits (red circles) to the spectra of Figs. 2–4, and the calculated values (green crosses) based on the average κ measured directly before and after each experiment. Unfortunately, κ is the main source of uncertainty in the theory curves, as it has a significant uncertainty from the OMIT fits and a spread (275−600 kHz) when measured directly from a laser wavelength scan before and after OMIT and PSD measurements. This is likely due to our imperfect stabilization of the laser to the cavity frequency, smeared out by the averaging. To illustrate, we have calculated the expected phase lag for a spread of $\kappa = 275-600$ kHz (green shaded area), all observed from measurements at the same wavelength and chip position. We have calculated the expected linewidths based on this spread using a model of a Fabry–Perot cavity with lossy membranes (Supplement 1 Sec. 8). There is reasonable agreement between the fitted and calculated values, and all values fall well within the band based on the spread in κ.

C. Cooperativity Competition

Independent of the optomechanical phase lag, we predict that if two mechanical resonators are coupled to the same optical field, the effective mechanical dissipation of one does not only depend on its local environment but also on the optomechanical cooperativity of the other resonator. We refer to this effect as *cooperativity competition* (for details see Supplement 1 Sec. 9). From the solution to Eq. (2), we can rewrite the position fluctuations in terms of the effective susceptibility $\chi_i^{\text{eff}}(\omega)$. We can further define the effective mechanical linewidths, which reduce to the simple expressions

$$\gamma_1^{\text{eff}} \approx \gamma_1 \left(1 + \frac{C_1}{C_2}\right), \quad \gamma_2^{\text{eff}} \approx \gamma_2 \left(1 + \frac{C_2}{C_1}\right). \tag{11}$$

Here, we assume identical mechanical frequencies and optimal cooling, $\Delta = \omega_1 = \omega_2$; side-band resolution, $\kappa \lesssim \omega_j$; and large optomechanical cooperativities, $C_j = 2G_j^2/(\kappa\gamma_j) \gg 1$. These equations describe how the effective mechanical dissipation of one resonator is reduced with respect to those of two independent modes, where $\gamma_j^{\text{eff}} \simeq \gamma_j(1 + C_j)$ $(j = 1, 2)$ [42–44]. While Eq. (11) describes a simplified model, for our experiments we use the full model (see Supplement 1 Sec. 9) to obtain γ_j^{eff}. Although both the optomechanical phase lag and the cooperativity competition originate from cavity-mediated coupling between the mechanical resonators, they are essentially different effects with their own characteristics, embodied by noise cancellation and competition in dissipation dynamics, respectively.

To observe cooperativity competition in our system, we vary cooperativities C_1 and C_2 [see Eq. (11)] by changing the coupling ratio $g_{0,1}/g_{0,2}$ or by changing the optical power. With $g_{0,1}/g_{0,2} = 0.74$ to keep the effect of the interference on the shape of our PSD constant, we measure at different powers [Fig. 4(a) (blue)]. The optomechanical parameters are determined as before, which we then use to fit our coupled (red) and independent (orange) models. The cooperativity competition manifests itself as a change in linewidth of the two resonances, which is difficult to gauge from the shape of the PSD, as it is dominated by the interference. Therefore, we have plotted the fitted linewidths in terms of the cooperativity in Fig. 4(b) for both the coupled case (solid curves), which contains both the interference and the cooperativity competition, and the independent case (dashed curve), which contains neither. This shows an appreciable reduction in linewidth for higher cooperativities as predicted.

We can further corroborate cooperativity competition by analyzing the fitted linewidths for various coupling ratios, shown in Fig. 4(c). We compare the total linewidth (sum of both linewidths) and expect a straight line as a function of C_1/C_2 in the independent case (orange, dashed), while cooperativity competition predicts a cooperativity-ratio-dependent reduction of the total linewidth (red, solid). The reduction is maximal when the cooperativities are approximately equal where the competition is most intense, and the curve is symmetric around $C_1/C_2 = 1$, which can be seen by

switching the labels 1, 2 of the resonators. The fitted linewidths are normalized to account for the cooling efficiency by rescaling the total linewidth by the maximum reduction expected due to cooperativity competition for the fitted κ, Δ, and cooperativities of each data point. The results match with the expected decrease associated with the cooperativity competition as a function of C_1/C_2. This shows the effective optomechanical coupling leading to a competition on the mechanical dissipation of the resonators.

4. CONCLUSION

We have introduced an optomechanical phase lag between the local and cavity-transduced thermal noises of the two resonators, originating from the time-delay of noise transduced via the cavity. We have observed interference stemming from this phase lag by measuring the mechanical power spectral density of a double-membrane device. The interference coherently cancels mechanical noise of the two resonators where their (broadened) frequency spectra overlap, leading to a 20 dB decrease in mechanical noise. This could create an interesting new method of controllably reducing unwanted mechanical noise by introducing a second resonator, which would allow cancellation of mechanical noise in a specific frequency range (Supplement 1, Sec. 10).

In addition, we have proposed and experimentally verified another new collective effect in the same system, where the effective susceptibility of the coupled resonators causes a competition on the mechanical dissipation. The dissipation rates of two mechanical resonators can get significantly reduced when their optomechanical cooperativities are comparable. This novel collective effect paves the way for long-range control of phonon dynamics [45], and the results of this work can be applied directly to multi-resonator ($N > 2$) optomechanical systems, where we expect more prominent and even richer collective effects.

Funding. Nederlandse Organisatie voor Wetenschappelijk Onderzoek (Frontiers of Nanoscience program, 680-47-541/994, 680-92-18-04); European Research Council (676842).

Acknowledgment. We thank João P. Moura and Klara Knupfer for their work in designing the cavity-membrane setup, and Girish S. Agarwal and David Vitali for helpful discussions.

Disclosures. The authors declare no conflicts of interest.

Data availability. All data, measurement, and analysis scripts in this work are available at [46].

Supplemental document. See Supplement 1 for supporting content.

[†]These authors contributed equally to this paper.

REFERENCES

1. M. Aspelmeyer, T. J. Kippenberg, and F. Marquardt, "Cavity optomechanics," Rev. Mod. Phys. **86**, 1391–1452 (2014).
2. Q. Lin, J. Rosenberg, D. Chang, R. Camacho, M. Eichenfield, K. J. Vahala, and O. Painter, "Coherent mixing of mechanical excitations in nano-optomechanical structures," Nat. Photonics **4**, 236–242 (2010).
3. F. Massel, S. U. Cho, J.-M. Pirkkalainen, P. J. Hakonen, T. T. Heikkilä, and M. A. Sillanpää, "Multimode circuit optomechanics near the quantum limit," Nat. Commun. **3**, 987 (2012).
4. A. B. Shkarin, N. E. Flowers-Jacobs, S. W. Hoch, A. D. Kashkanova, C. Deutsch, J. Reichel, and J. G. E. Harris, "Optically mediated hybridization between two mechanical modes," Phys. Rev. Lett. **112**, 013602 (2014).
5. C. F. Ockeloen-Korppi, M. F. Gely, E. Damskägg, M. Jenkins, G. A. Steele, and M. A. Sillanpää, "Sideband cooling of nearly degenerate micromechanical oscillators in a multimode optomechanical system," Phys. Rev. A **99**, 023826 (2019).
6. M. Zhang, G. S. Wiederhecker, S. Manipatruni, A. Barnard, P. McEuen, and M. Lipson, "Synchronization of micromechanical oscillators using light," Phys. Rev. Lett. **109**, 233906 (2012).
7. M. Bagheri, M. Poot, L. Fan, F. Marquardt, and H. X. Tang, "Photonic cavity synchronization of nanomechanical oscillators," Phys. Rev. Lett. **111**, 213902 (2013).
8. J. Sheng, X. Wei, C. Yang, and H. Wu, "Self-organized synchronization of phonon lasers," Phys. Rev. Lett. **124**, 053604 (2020).
9. M. J. Weaver, F. Buters, F. Luna, H. Eerkens, K. Heeck, S. de Man, and D. Bouwmeester, "Coherent optomechanical state transfer between disparate mechanical resonators," Nat. Commun. **8**, 824 (2017).
10. N. Spethmann, J. Kohler, S. Schreppler, L. Buchmann, and D. M. Stamper-Kurn, "Cavity-mediated coupling of mechanical oscillators limited by quantum back-action," Nat. Phys. **12**, 27–31 (2016).
11. H. Xu, D. Mason, L. Jiang, and J. G. E. Harris, "Topological energy transfer in an optomechanical system with exceptional points," Nature **537**, 80–83 (2016).
12. I. Mahboob, H. Okamoto, K. Onomitsu, and H. Yamaguchi, "Two-mode thermal-noise squeezing in an electromechanical resonator," Phys. Rev. Lett. **113**, 167203 (2014).
13. A. Pontin, M. Bonaldi, A. Borrielli, L. Marconi, F. Marino, G. Pandraud, G. A. Prodi, P. M. Sarro, E. Serra, and F. Marin, "Dynamical two-mode squeezing of thermal fluctuations in a cavity optomechanical system," Phys. Rev. Lett. **116**, 103601 (2016).
14. C. F. Ockeloen-Korppi, E. Damskägg, J.-M. Pirkkalainen, M. Asjad, A. A. Clerk, F. Massel, M. J. Woolley, and M. A. Sillanpää, "Stabilized entanglement of massive mechanical oscillators," Nature **556**, 478–482 (2018).
15. A. Xuereb, C. Genes, and A. Dantan, "Strong coupling and long-range collective interactions in optomechanical arrays," Phys. Rev. Lett. **109**, 223601 (2012).
16. J. Li, A. Xuereb, N. Malossi, and D. Vitali, "Cavity mode frequencies and strong optomechanical coupling in two-membrane cavity optomechanics," J. Opt. **18**, 084001 (2016).
17. P. Piergentili, L. Catalini, M. Bawaj, S. Zippilli, N. Malossi, R. Natali, D. Vitali, and G. Di Giuseppe, "Two-membrane cavity optomechanics," New J. Phys. **20**, 083024 (2018).
18. D. C. Newsom, F. Luna, V. Fedoseev, W. Löffler, and D. Bouwmeester, "Optimal optomechanical coupling strength in multimembrane systems," Phys. Rev. A **101**, 033829 (2020).
19. G. Heinrich, M. Ludwig, J. Qian, B. Kubala, and F. Marquardt, "Collective dynamics in optomechanical arrays," Phys. Rev. Lett. **107**, 043603 (2011).
20. M. J. Woolley and A. A. Clerk, "Two-mode squeezed states in cavity optomechanics via engineering of a single reservoir," Phys. Rev. A **89**, 063805 (2014).
21. J. Li, I. M. Haghighi, N. Malossi, S. Zippilli, and D. Vitali, "Generation and detection of large and robust entanglement between two different mechanical resonators in cavity optomechanics," New J. Phys. **17**, 103037 (2015).
22. L. F. Buchmann and D. M. Stamper-Kurn, "Nondegenerate multimode optomechanics," Phys. Rev. A **92**, 013851 (2015).
23. T. Kipf and G. S. Agarwal, "Superradiance and collective gain in multimode optomechanics," Phys. Rev. A **90**, 053808 (2014).
24. H. Seok, L. F. Buchmann, S. Singh, and P. Meystre, "Optically mediated nonlinear quantum optomechanics," Phys. Rev. A **86**, 063829 (2012).
25. V. Fedoseev, F. Luna, W. Löffler, and D. Bouwmeester, "Stimulated Raman adiabatic passage in optomechanics," Phys. Rev. Lett. **126**, 113601 (2021).
26. S. Stassi, A. Chiado, G. Calafiore, G. Palmara, S. Cabrini, and C. Ricciardi, "Experimental evidence of Fano resonances in nanomechanical resonators," Sci. Rep. **7**, 1065 (2017).
27. J. M. Dobrindt and T. J. Kippenberg, "Theoretical analysis of mechanical displacement measurement using a multiple cavity mode transducer," Phys. Rev. Lett. **104**, 033901 (2010).
28. Y. Yanay, J. C. Sankey, and A. A. Clerk, "Quantum backaction and noise interference in asymmetric two-cavity optomechanical systems," Phys. Rev. A **93**, 063809 (2016).
29. T. Caniard, P. Verlot, T. Briant, P.-F. Cohadon, and A. Heidmann, "Observation of back-action noise cancellation in interferometric and weak-force measurements," Phys. Rev. Lett. **99**, 110801 (2007).

30. C. Gärtner, J. P. Moura, W. Haaxman, R. A. Norte, and S. Gröblacher, "Integrated optomechanical arrays of two high reflectivity SiN membranes," Nano Lett. **18**, 7171–7175 (2018).
31. R. A. Norte, J. P. Moura, and S. Gröblacher, "Mechanical resonators for quantum optomechanics experiments at room temperature," Phys. Rev. Lett. **116**, 147202 (2016).
32. A. M. Jayich, J. C. Sankey, B. M. Zwickl, C. Yang, J. D. Thompson, S. M. Girvin, A. A. Clerk, F. Marquardt, and J. G. E. Harris, "Dispersive optomechanics: a membrane inside a cavity," New J. Phys. **10**, 095008 (2008).
33. E. D. Black, "An introduction to Pound-Drever-Hall laser frequency stabilization," Am. J. Phys. **69**, 79 (2001).
34. D. Boyanovsky and D. Jasnow, "Coherence of mechanical oscillators mediated by coupling to different baths," Phys. Rev. A **96**, 012103 (2017).
35. R. Benguria and M. Kac, "Quantum Langevin equation," Phys. Rev. Lett. **46**, 1 (1981).
36. V. Giovannetti and D. Vitali, "Phase-noise measurement in a cavity with a movable mirror undergoing quantum Brownian motion," Phys. Rev. A **63**, 023812 (2001).
37. U. Fano, "Effects of configuration interaction on intensities and phase shifts," Phys. Rev. **124**, 1866–1878 (1961).
38. S. Weis, R. Rivière, S. Deléglise, E. Gavartin, O. Arcizet, A. Schliesser, and T. J. Kippenberg, "Optomechanically induced transparency," Science **330**, 1520–1523 (2010).
39. G. S. Agarwal and S. Huang, "Electromagnetically induced transparency in mechanical effects of light," Phys. Rev. A **81**, 041803 (2010).
40. W. H. P. Nielsen, Y. Tsaturyan, C. B. Møller, E. S. Polzik, and A. Schliesser, "Multimode optomechanical system in the quantum regime," Proc. Natl. Acad. Sci. USA **114**, 62–66 (2017).
41. R. A. Rodrigues, "Fano-like antiresonances in nanomechanical and optomechanical systems," Phys. Rev. Lett. **102**, 067202 (2009).
42. I. Wilson-Rae, N. Nooshi, W. Zwerger, and T. J. Kippenberg, "Theory of ground state cooling of a mechanical oscillator using dynamical backaction," Phys. Rev. Lett. **99**, 093901 (2007).
43. F. Marquardt, J. P. Chen, A. A. Clerk, and S. M. Girvin, "Quantum theory of cavity-assisted sideband cooling of mechanical motion," Phys. Rev. Lett. **99**, 093902 (2007).
44. C. Genes, D. Vitali, P. Tombesi, S. Gigan, and M. Aspelmeyer, "Ground-state cooling of a micromechanical oscillator: Comparing cold damping and cavity-assisted cooling schemes," Phys. Rev. A **77**, 033804 (2008).
45. A. Xuereb, C. Genes, G. Pupillo, M. Paternostro, and A. Dantan, "Reconfigurable long-range phonon dynamics in optomechanical arrays," Phys. Rev. Lett. **112**, 133604 (2014).
46. M. De Jong, J. Li, C. Gärtner, R. Norte, and S. Gröblacher, "Data from: Coherent mechanical noise cancellation and cooperativity competition in optomechanical arrays," Zenodo, 2021, https://doi.org/10.5281/zenodo.5782970.